Calibrations of filter radiometers for determination of atmospheric optical depth

Ch. Wehrli

Abstract. Atmospheric optical depths are determined by relating ground-based measurements of direct solar radiation to the extraterrestrial value, I_0, that a filter radiometer would read outside the atmosphere. Usually I_0 is determined by the Langley extrapolation technique from a high-altitude site, where clear and highly stable atmospheric conditions may be found. Alternatively, I_0 can be measured *in situ* from a stratospheric balloon experiment. We have employed both methods and found agreement to better than 1%. Filter radiometers tend to change over time, especially when used operationally outdoors. Absolute calibrations in the laboratory are used to monitor the radiometric stability of filter radiometers at the Physikalisch-Meteorologisches Observatorium Davos (PMOD/WRC, Switzerland). A spectral calibration facility based on a calibrated trap detector from the Physikalisch-Technische Bundesanstalt (PTB, Germany) is used to relate the filter radiometer to an accurate and long-term traceable standard. An FEL-lamp-based standard, previously used for several years, was compared with the new trap standard via a filter radiometer at four wavelengths between 368 nm and 862 nm and revealed a systematic difference of the order of 5%. The link between radiometric and I_0 calibration is the value of the extraterrestrial solar spectrum at the filter radiometer wavelengths which can be determined from these two calibrations and compared with published values.

1. Introduction

Atmospheric aerosols play an important role in the Earth's radiation budget and thus in climatic change through their direct and indirect effects: these may be as large as, but opposite in sign to, the effect of increased CO_2 concentration. However, owing to their high spatial and temporal variability (seasonal dust storms or biomass burning), their globally and annually averaged climatic forcing is associated with a large uncertainty. Aerosol optical depth (AOD) is a key quantity describing the combined effects of scattering and absorption of radiation by aerosols within the atmosphere. Wavelength-dependent AOD can be determined from extinction measurements of direct sunlight according to the Beer-Bouger-Lambert law for monochromatic radiation:

$$I(\lambda) = I_0(\lambda)/R^2 \exp[-\tau(\lambda)m], \quad (1)$$

where $I_0(\lambda)$ is the incident flux at the mean Sun-Earth distance of one astronomical unit (AU) and $I(\lambda)$ is the flux transmitted through a homogeneous layer of optical depth $\tau(\lambda)$ R is the Sun-Earth distance in astronomical units, m is the geometric path length, "air mass" in meteorological terminology. For a plane parallel atmosphere, m is equal to $\sec(\zeta)$ with ζ being the solar zenith angle; for realistic atmospheres more complex formulas are used.

The AOD $\tau_a(\lambda)$ is determined as the difference between total and Rayleigh scattering, $\tau_R(\lambda)$ and gas absorption, $\tau_a(\lambda)$ optical depths:

$$\tau_a(\lambda) = \log[I(\lambda)R^2/I_0(\lambda)]/m - \tau_R(\lambda) - \tau_g(\lambda) \quad (2)$$

Wavelengths are chosen in spectral bands where gas absorption is negligible or absent. The World Meteorological Organization has recommended a set of wavelengths to be used for AOD determinations.

2. Precision filter radiometer

For at least forty years filter radiometers have been used in meteorology for the determination of atmospheric haze or turbidity. Modern sun-photometers use dielectric interference filters and silicon photodetectors resembling the filter radiometers used in metrology. A new generation of sun-photometers, precision filter radiometers (PFRs), has been designed with emphasis on radiometric stability and a small number of instruments were built for a trial network of AOD

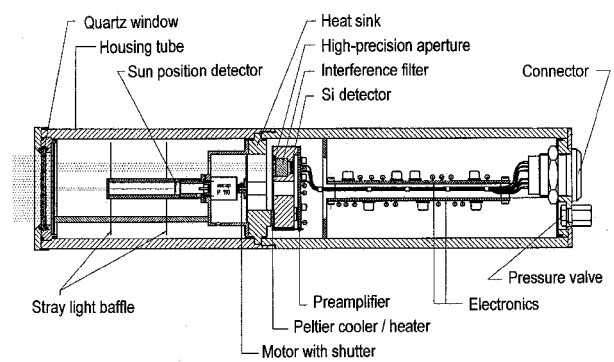

Figure 1. Schematic diagram of precision filter radiometer. Mechanical: diameter 88 mm, length 390 mm, mass 3 kg. Optical: four channels at 862 nm, 500 nm, 412 nm and 368 nm with 5 nm FWHM bandwidth; field-of-view 2.5°, slope angle 0.7°.

Ch. Wehrli: Physikalisch-Meteorologisches Observatorium Davos/World Radiation Center (PMOD/WRC), Dorfstrasse 33, 7260 Davos Dorf, Switzerland.

measurement sites. Figure 1 is a schematic diagram of the PFR with key specifications. The interference filters are manufactured using an ion-assisted deposition technology. The silicon photodiodes, tilted at an angle of 3° from the optical axis to reduce interreflections, are operated in photovoltaic mode. Four radiometric channels are mounted in a common detector head, whose temperature is maintained at (20±0.1)°C by a Peltier-type thermostatic controller. The filters are thus not subjected to diurnal temperature cycling when operated outdoors. An internal shutter opens for only a few seconds every 2 min during actual measurements in order to keep exposure-related degradation to a minimum.

3. Top-of-the-atmosphere (TOA) calibration

The calibration constant, $I_0(\lambda)$ of a sun-photometer is the signal it would read on top of the atmosphere at mean Sun-Earth distance. It is commonly determined by Langley extrapolation of several measurements, taken at different solar zenith angles or air masses, to air mass zero. Alternatively, $I_0(\lambda)$ can be determined *in situ* from a stratospheric balloon or rocket platform as described by Wehrli and Fröhlich [1].

3.1 Langley method

A number of irradiance measurements, $I(\lambda)$ taken at different solar zenith angles can be least-squares-fitted to (1) and solved for $I_0(\lambda)$ and $\tau(\lambda)$ a procedure that is commonly known as Langley calibration. The underlying assumption, that the atmosphere is temporarily and spatially stable during the measurement period, is seldom fulfilled below the atmospheric boundary layer; thus Langley calibrations are often performed at high-altitude sites. Because the air mass, m, depends not only on solar zenith angle but also on the vertical distribution of the attenuating components, a refined method taking into account different air masses for the different components is sometimes used. For a more detailed description see, for example, Schmid and Wehrli [2].

Several PFR instruments were operated at Jungfraujoch (46.55° N., 7.99° E., 3580 m above sea level) in a fully automated station of the Swiss Meteorological Institute. During a period of clear winter days, between 15 December 1998 and 25 February 1999, a series of 22 refined Langley calibrations with either decreasing or increasing solar zenith angles was made for instrument PFRN2. A subset of 17 of these calibrations was selected that covered an air mass range of at least 2 with more than 20 data points and had a relative standard deviation of the extrapolated $I_0(\lambda)$ of less than 1 %. Their average and standard deviations are shown in Table 1 in the "N2 Langley" row and the following row.

Table 1. Comparison of Langley and *in situ* extraterrestrial calibrations of two filter radiometers.

	Wavelength/nm			
	862	500	412	368
N1 *in situ*	3.350	3.751	3.600	4.055
Uncertainty	0.004	0.002	0.006	0.010
Ratio N2/N1	1.0129	1.0029	1.0222	0.9610
Standard deviation	0.0006	0.0004	0.0003	0.0004
N2 *in situ*	3.393	3.762	3.680	3.897
N2 Langley	3.418	3.767	3.705	3.929
Standard deviation	0.003	0.004	0.003	0.005
Langley/*in situ*	**1.0073**	**1.0014**	**1.0068**	**1.0082**

3.2 Stratospheric balloon flight

On 22 October 1998 the stratospheric balloon experiment SIMBA98 was launched from Aire-sur-l'Adour in southern France. The balloon briefly reached a ceiling altitude of 39.5 km before the Sun reached its zenith angle, ζ, of 55°. Measurements of solar irradiance were taken during the 70 min before the gondola was separated from the balloon. A more detailed description of the SIMBA98 experiment is given in Anklin et al. [3].

The measurements taken from the balloon with instrument PFRN1 need to be corrected for extinction by the residual atmosphere above the gondola. This can be done by numerical modelling as a function of height and solar zenith angle. The flight trajectory was measured continuously in latitude, longitude and altitude by an on-board Global Positioning System. Corresponding solar zenith angles and Sun-Earth distances were calculated using an ephemeris algorithm.

A look-up table of atmospheric transmissions was calculated using MODTRAN 3.7 [4] code for three zenith angles at 54°, 56° and 58° and eight altitudes between 34.5 km and 40.5 km. The 1976 US standard atmosphere model was used in a modified version that provides finer altitude resolution above 30 km. Average transmission values at ceiling altitude were between 0.9966 for the 368 nm and 0.9997 for the 862 nm channel, with uncertainties of less than 0.001.

The corrected signals show systematic trends of the order of a few parts times 10^{-3}, with wavelength-dependent rates and signs hinting at an accelerated ageing effect owing to increased ultraviolet (UV) flux at 40 km. The resulting I_0 values, normalized to a Sun-Earth distance of 1 AU, and their estimated uncertainties are listed in Table 1 under "N1 *in situ*".

3.3 Comparison of TOA calibrations

Both instruments, PFRN1 and PFRN2, were operated synchronously at Davos on 24 March 1999. Their signal ratio PFRN2/PFRN1 is used to transfer an "N1 *in situ*" to an "N2 *in situ*" value that is compared with the Langley calibrations of PFRN2. The two methods of TOA calibration agree to better than 1 % and are within their combined standard deviations.

4. Absolute calibration

The radiometric stability of I_0 calibrated PFRs is monitored by absolute calibration against the PTB cryogenic radiometer scale via a calibrated trap detector. A classic FEL-lamp calibration is used to verify the newly implemented trap-calibration method. As the PFR viewing geometry is designed for solar

measurements, the front part containing the view-limiting and stray-light apertures has to be replaced by baffles in the laboratory set-up. The quartz window is replaced by an identical window mounted close to the radiometric apertures.

4.1 Trap-detector-based calibration

A spectral comparator facility, similar to the one at the PTB-Berlin described by Friedrich et al. [5], is used. The trap detector was calibrated by the PTB in spring 1998 at twelve laser wavelengths between 356.4 nm and 899.8 nm with a relative uncertainty of less than 5×10^{-4} at 356 nm and less than 10^{-4} above 476 nm. A cubic spline interpolation is used between calibration points. Taking a possible ageing of the trap detector into account, the relative uncertainty above 400 nm will probably not exceed our goal of 10^{-3}, but may be as high as 2.5×10^{-3} in the UV range.

Figure 2 shows the optical set-up of the spectral calibration facility. Light from either a tungsten-halogen or a xenon-arc lamp, L, is imaged on to the entrance slit of a grating monochromator with a focal length of 640 mm via a light chopper, CH. A small solid-state laser is used during alignment of the detectors on to the optical axis. The monochromator has a linear dispersion of 1.2 nm per millimetre slit width and a wavelength accuracy of 0.05 nm. The wavelength scale was verified using spectral lamps and a He-Ne laser. The spherical mirror M3 forms an astigmatic image of the 0.5 mm × 0.5 mm exit slit at the aperture plane of the detectors. A PFR radiometric aperture is mounted in front of the trap detector and all aperture areas are accurately determined by optical flux

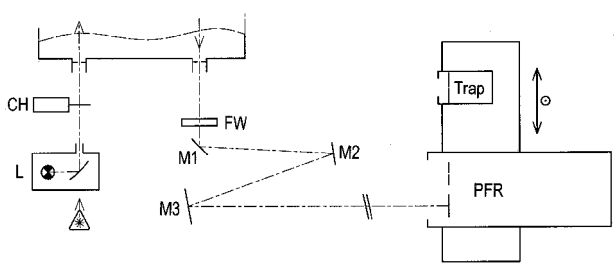

Figure 2. Optical set-up of spectral calibration facility.

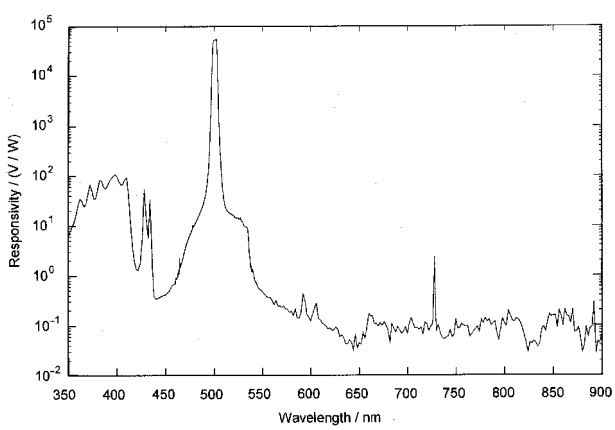

Figure 3. Spectral responsivity for 500 nm channel.

Table 2. Response integrals for PFRN001 calibrations/(V mW^{-1}).

	Wavelength/nm			
Date	862	500	412	368
1998-08-20	484.23	273.87	290.70	477.36
1999-03-15	486.66	273.45	291.52	483.61
1999-09-21	480.12	272.19	287.98	478.65

comparison with a reference aperture measured at the UK National Physical Laboratory [6]. The apertures are underfilled to avoid homogeneity problems, and flux rather than irradiance is compared. Schott glass filters, FW, are used to suppress higher orders of the single-pass monochromator. The PFR instrument and the trap detector are mounted on an industrial-grade, two-axis translation stage that can move rapidly between detectors with a repeatability of 20 μm.

4.1.1 Measurements

A wavelength range of ±50 nm around the nominal centre wavelength of the filter radiometer is scanned in 0.5 nm steps. At each wavelength, the signals from both detectors are measured four times by a digital lock-in amplifier voltmeter. The response measurements are noise-limited by the filter radiometer amplifiers.

Out-of-band rejection was measured with monochromator slits opened to 2 mm × 2 mm, slightly overfilling the detector apertures. While the two UV channels had no detectable response in the range 330 nm to 1080 nm, the 500 nm and 862 nm channels showed spectral leaks of $<10^{-3}$ of their peak response.

Instrument N1 was calibrated three times: on 20 August 1998 and 15 March 1999 with a tungsten-halogen lamp, and on 21 September 1999 with a xenon-arc source. For the last calibration, nine to twelve spectral scans were averaged to achieve the dynamic range shown in Figure 3. Integrals were calculated over wavelength intervals where the response is larger than 0.001 times the peak value. The standard deviation of these multiple-scan integrals is of the order of a few times 10^{-4}. Table 2 shows that all four channels are stable within 1%. No significant trend larger than the set-up reproducibility of the order of 0.5% could be detected.

4.2 FEL-lamp calibration

Two FEL-type secondary standard lamps, calibrated by EG&G on the US National Bureau of Standards 1973 scale in June 1983 and March 1991, were used. Lamp #240 had 74 h and lamp #862 had 19 h of operation in January 1999: no correction for ageing is applied. Irradiance values are interpolated between tabulated values $E(\lambda)$ and reciprocal wavelength using a linearized black-body approximation

$$\ln[E(\lambda)\lambda^5] \approx \ln(C_1) - C_2/T\lambda^{-1}. \quad (3)$$

The set-up and measurement procedures were described in an earlier publication [1] where the absolute uncertainty was estimated to be between

Table 3. Ratios of expected to measured lamp signals of absolute calibrations in September 1999.

	Wavelength/nm			
	862	500	412	368
I_{exp}/V	0.776	0.148	0.057	0.044
I_{meas}/V	0.817	0.155	0.060	0.046
Ratio	0.950	0.952	0.949	0.956

Table 4. Ratios of extraterrestrial signals expected from absolute calibrations and solar spectra to signals measured from balloon (symbols explained in text).

	Wavelength/nm				
	862	500	412	368	Ave
TW	1.003	0.971	0.977	1.023	0.994
TM	0.990	0.963	0.986	1.055	0.999
LW	1.053	1.028	1.032	1.068	1.045

1.9% in the infrared and 2.7% in the UV spectral ranges. However, in a comparison of eighteen lamps Kiedron et al. [7] have found deviations twice as large for individual lamps. The longwave out-of-band contribution was estimated by cut-off filter measurements to be about 4% at 368 nm, 1% at 412 nm and <0.1% at 500 nm; the 862 nm channel could not be tested owing to lack of suitable filters.

A calibration factor, $C(\lambda)$ for the filter radiometer is calculated by dividing the measured signal, V_L, by the mean lamp spectral irradiance, weighted by the filter bandpass. PFRN1 was calibrated four times, on 29 April 1998, and 8 March, 29 July and 9 October 1999. The calibration factors determined from both lamps always differed by less than 0.7%, except in one case where they were 1.42% apart. Contrary to the response integrals, the lamp calibration factors tend to increase with time, at annual rates from 1.1% at 412 nm to 1.5% at 500 nm.

4.3 Comparison between absolute calibrations and with solar irradiance spectrum

The trap-calibrated responsivity, $R(\lambda)$ can be used to calculate an expected signal, I_{exp}, that the filter radiometer would measure during lamp calibration and then compare with the signal I_{meas}, actually measured:

$$I_{exp} = A \int R(\lambda) E(\lambda) d\lambda, \quad (4)$$

where A is the measured radiometric aperture area and $E(\lambda)$ is the interpolated lamp irradiance. Table 3 shows a systematic, largely wavelength-independent, difference of about 5% between lamp- and trap-based methods. In order to judge whether the lamp or the trap calibrations are in error, both can be used to estimate expected extraterrestrial signals I_{exp} via a solar spectrum, which can then be compared with the I_0 measured by the balloon experiment. As in (4), the responsivity is now multiplied with either the WRC85 [8] or the MODTRAN 3.7 [4] spectrum, which have estimated relative uncertainties of about 2×10^{-2} in the spectral range considered. Lamp calibration factors are multiplied by the bandpass-weighted average solar spectrum as described in [1]. Row TW in Table 4 uses trap responsivities with spectrum [8], TM with spectrum [4], while LW uses lamp calibration factors and spectrum [8]. The last column gives the wavelength average. Clearly the lamp calibration systematically overestimates the SIMBA98 values by about 4.5%, while the trap calibration both over- and underestimates, and agrees on average within better than 1% with the balloon results.

5. Conclusions

Results from a stratospheric balloon experiment have confirmed the extraterrestrial calibration, I_0, of filter radiometers by refined Langley extrapolation from the Jungfraujoch observatory to better than 1%. At this level of uncertainty, the two methods may thus be considered equivalent.

Absolute calibrations by a newly implemented trap-detector-based facility have demonstrated the stability of a reference filter radiometer within 1% over one year. Further improvement of the facility is needed to achieve a set-up reproducibility of better than ±0.5%.

Calibrations by two FEL standard lamps show drifts of 1% to 2% over 17 months and an unexpected, systematic difference of 5% with respect to the trap calibration. A comparison via a solar spectrum suggests that the lamp irradiances are overestimated. A recalibration of the lamps to the US National Institute of Standards and Technology 1990 scale and further investigations into possible causes, including out-of-band transmission, are needed to reduce this difference in absolute calibrations.

Acknowledgements. The author gratefully acknowledges Drs J. Fischer and L. Werner of the PTB for calibration of the trap detector; Dr A. Heimo of the SMA for providing access to the facilities at Jungfraujoch and U. Schütz of the PMOD/WRC for programming the laboratory data acquisition.

References

1. Wehrli Ch., Fröhlich C., *Metrologia*, 1991, **28**, 285-289.
2. Schmid B., Wehrli Ch., *Appl. Opt.*, 1995, **34**, 4500-4512.
3. Anklin M., Wehrli Ch., Fröhlich C., Pepe F., In *Proc. 14th ESA Symp. European rocket and balloon programmes and related research*, ESA SP-437, Noordwijk, the Netherlands, European Space Agency ESTEC, 1999.
4. Acharya P. K. et al., *MODTRAN Version 3.7/4.0 Users' Manual*, Air Force Research Laboratory, Hanscom AFB, MA 01731-3010, USA, 1998.
5. Friedrich R., Fischer J., Stock M., *Metrologia*, 1995/96, **32**, 509-513.
6. Martin J. E., Fox N. P., Harrison N. J., Shipp B., Anklin M., *Metrologia*, 1998, **35**, 461-464.
7. Kiedron P. W., Michalsky J. J., Berndt J. L., Harrison L. C., *Appl. Opt.*, 1999, **38**, 2432-2439.
8. Wehrli C., PMOD publication No. 615, Davos Dorf, Physikalisch-Meteorologisches Observatorium Davos, 1985.